Check for updates

Accepted Article

Unveiling the Morphological and Physical Mechanism of Burn-in Loss Alleviation by Ternary Matrix Towards Stable and Efficient All-Polymer Solar Cells

Ruijie Ma, Qunping Fan*, Top Archie Dela Peña, Baohua Wu, Heng Liu, Qiang Wu, Qi Wei, Jiaying Wu, Xinhui Lu, Mingjie Li, Wei Ma*, Gang Li*

Dr. Ruijie Ma, Prof. Gang Li

Department of Electronic and Information Engineering, Research Institute for Smart Energy (RISE), Guangdong-Hong Kong-Macao (GHM) Joint Laboratory for Photonic-Thermal-Electrical Energy Materials and Devices, The Hong Kong Polytechnic University, Hung Hom, Kowloon, Hong Kong, 999077, China

Email: gang.w.li@polyu.edu.hk

Prof. Qunping Fan, Baohua Wu, Dr. Qiang Wu, Prof. Wei Ma

State Key Laboratory for Mechanical Behavior of Materials, Xi'an Jiaotong University, Xi'an 710049, China

Email: qunping@xjtu.edu.cn; msewma@xjtu.edu.cn

Top Archie Dela Peña, Dr. Qi Wei, Prof. Mingjie Li

Department of Applied Physics, The Hong Kong Polytechnic University, Hong Kong, China

Heng Liu, Prof. Xinhui Lu

This article has been accepted for publication and undergone full peer review but has not been through the copyediting, typesetting, pagination and proofreading process, which may lead to differences between this version and the Version of Record. Please cite this article as doi: 10.1002/adma.202212275.

This article is protected by copyright. All rights reserved.

15214095, ja, Downloaded from https://onlinelibrary.wiley.com/doi/10.1002/adma.202212275 by Hong Kong Poly University, Wiley Online Library on [10/02/2023]. See the Terms and Conditions (https://onlinelibrary.wiley.com/terms-and-conditions) on Wiley Online Library for rules of use; OA articles are governed by the applicable Creative Commons License

Accepted Article

Department of Physics, Chinese University of Hong Kong, Hong Kong, New Territories Hong Kong 999077, China

Top Archie Dela Peña, Prof. Jiaying Wu

Advanced Materials Thrust, Function Hub, The Hong Kong University of Science and Technology, Nansha, Guangzhou, Guangdong, China

Abstract

All-polymer solar cells (All-PSCs) are considered the most promising candidate in achieving both efficient and stable organic photovoltaic devices, yet the field has rarely presented in-depth understanding of corresponding device stability while efficiency is continuously boosted via the innovation of polymer acceptors. Herein, we build a ternary matrix for all-PSCs with optimized morphology, improved film ductility and importantly, boosted efficiency and better operational stability than its parental binary counterparts, as a platform to study the underlying mechanism. The target system PQM-Cl:PTQ10:PY-IT (0.8:0.2:1.2) exhibits an alleviated burn-in loss of morphology and efficiency under light soaking, which supports its promoted device lifetime. The comprehensive characterizations of fresh and light-soaked active layers lead us to a clear illustration of opposite morphological and physical degradation direction of PQM-Cl and PTQ10, thus resulting in a delicate balance at the optimal ternary system. Specifically, the enlarging tendency of PQM-Cl and shrinking preference of PTQ10 in terms of phase separation leads to a stable morphology in their mixing phase; the hole transfer kinetics of PQM-Cl:PY-IT host is stabilized by incorporating PTQ10. This work succeeds in reaching a deep insight of all-PSC's stability promotion by a rational ternary design, which booms the prospect of gaining high-performance all-PSCs.

Key words: all-polymer solar cells, stability, ternary matrix, burn-in loss reduction, understanding

This article is protected by copyright. All rights reserved.

15214095, ja, Downloaded from https://onlinelibrary.wiley.com/doi/10.1002/adma.202212275 by Hong Kong Poly University, Wiley Online Library on [10/02/2023]. See the Terms and Conditions (https://onlinelibrary.wiley.com/terms-and-conditions) on Wiley Online Library for rules of use; OA articles are governed by the applicable Creative Commons License

Accepted Article

Introduction

All-polymer solar cell (All-PSC) is considered to be the most promising organic photovoltaic (OPV) technology in practical applications, due to the excellent morphological stability and mechanical durability, compared with the small molecule composed counterparts.[1-5] However, the power conversion efficiency (PCE) values of all-PSCs have suffered a long-term poor performance, due to the insufficient donor-acceptor intermixing (results in weak free exciton generation) and mediocre crystallization (leads to low charge transport), until polymerized small-molecule-acceptor (PSMA) is proposed.[6-10] To date, the rapid development of pushing the efficiency of all-PSCs over 17% demonstrates new vitality in this research field.[11-16]

Current research mainstream of all-PSCs is to further promote the PCEs as high as those of small molecule composed counterparts,[17-21] and empirically the ternary blend strategy is one of the most commonly used methods to achieve this goal.[22-28] Notably, these works also prefer to claim an enhanced device stability and sometimes better mechanical durability, but very few works provide in-depth understanding for such improvements.[29-31] Since the chemical nature of PSMAs now has altered from those traditional perylene diimide (PDI) and naphthalene diimide (NDI) based ones to small molecule based ones, the variation of device stability deserves more insightful investigation, instead of being an attached parameter reported along with PCE promoted by ternary matrix design.

In term of stability enhancement, one of the most effective ways is to reduce the burn-in loss of morphology and OPV devices.[32-34] Apart from widely acknowledged mechanism of trap-assisted recombination increase, the morphology degradation (especially mixing or de-mixing of donor and acceptor) is found to be an important factor, as well.[35,36] Since both evolution behaviors could result in significant burn-in loss, finding a balance point to

This article is protected by copyright. All rights reserved.

15214095, ja, Downloaded from https://onlinelibrary.wiley.com/doi/10.1002/adma.202212275 by Hong Kong Poly University, Wiley Online Library on [10/02/2023]. See the Terms and Conditions (https://onlinelibrary.wiley.com/terms-and-conditions) on Wiley Online Library for rules of use; OA articles are governed by the applicable Creative Commons License

Accepted Article

minimize the undesired morphology degradation is supposed to be a good choice. Thereby, mixing two efficient binary donor-acceptor systems with different phase evolution directions is expected to be a rational and practical ternary strategy to obtain efficient and stable OPV devices. In addition, correlating the device performance, active layer morphology and physics parameters of all-PSCs is beneficial to understanding the stability variation, but not yet paid enough attention.

Here, two parental binary all-polymer systems of PQM-Cl:PY-IT and PTQ10:PY-IT[37-40] are selected to construct high-performance ternary blend. The optimal ternary PQM-Cl:PTQ10:PY-IT (0.8:0.2:1.2) blend achieves a champion PCE of 18.45% in all-PSCs due to the systematically enhanced open-circuit voltage (V_{OC}), short-circuit current density (J_{SC}) and fill factor (*FF*), with the film ductility rises up simultaneously. More importantly, the optimized ternary all-PSCs obtain significantly enhanced device operation stability under maximal power point (MPP) tracking, compared with their counterparts of other component ratios, mainly due to the alleviation of burn-in degradation. On the basis of such variation of component ratios, the devices with active layers degraded for 10 hours under 1-sun illumination in N_2 glovebox are fabricated, and the results further support the burn-in loss minimization in optimal ternary blend. Morphological characterizations present a well-kept phase separation in optimal ternary film after strong photo stress, while other systems deviate from their own initial state. As for crystallinity behavior, the face-on orientation and π–π stacking ordering is also best maintained in optimal ternary blend. Considering the parameters of all other systems, PTQ10's morphology degradation direction is opposite to that of PQM-Cl, which probably enables a desired balance when the blend ratio is 0.8:0.2:1.2. Furthermore, photo-physics experiments unveil a charge transfer pathway from PTQ10 to PQM-Cl, which also acts as additional charge generation channel, protected PQM-Cl charge generation features in donor blend, and well-kept hole transfer kinetics in optimal ternary system after light soaking as a result of opposite variation directions in PQM-Cl:PY-IT and

This article is protected by copyright. All rights reserved.

15214095, ja, Downloaded from https://onlinelibrary.wiley.com/doi/10.1002/adma.202212275 by Hong Kong Poly University, Wiley Online Library on [10/02/2023]. See the Terms and Conditions (https://onlinelibrary.wiley.com/terms-and-conditions) on Wiley Online Library for rules of use; OA articles are governed by the applicable Creative Commons License

Accepted Article

PTQ10:PY-IT binary films cancelling each other out. This work clearly presents the meaning of rational ternary design to increase device stability supported by comprehensive morphological and physical investigations, boosting the prospect of constructing all-PSCs with decent performance parameters.

Results and Discussion

Figure 1a presents the chemical structures of target polymers of PQM-Cl, PTQ10, and PY-IT. Here we assess the energy level landscape of three polymers based on literatures, [38,40] where we can learn that PTQ10 has a deeper highest occupied molecular orbital (HOMO) energy level than PQM-Cl, suggesting introducing PTQ10 as the third could increase V_{OC}. Subsequently, the normalized ultraviolet-visible (UV-vis) absorption spectra of both neat and blend films are given in **Figure S1**. PQM-Cl and PTQ10 display complementary absorption profiles, indicative of more efficient charge generation could be achieved when these two materials are combined, which would be discussed later. Compared with the donor-only and acceptor-only absorption profile in **Figure S1a**, those blend films in **Figure S1b** show different peak shapes for PQM-Cl and PTQ10 and well-kept peak shapes for PY-IT. These results imply the aggregation of donor materials will be tuned when blending with PY-IT, which is to say that PY-IT dominates the competition in film morphology. To be specific, the height of 0-0 vibrational peak for PQM-Cl becomes lower than 0-1 vibrational peak in blend, although it is higher in the pure film. This phenomenon exists in all PQM-Cl-based blend film *vs* donor-only film pairs, so blending these PQM-Cl and PY-IT can suppress the *J*-aggregation and enhance the *H*-aggregation of donor, providing additional hole transport channels along in-plane direction, while the efficient out-of-plane directional electron transport is guaranteed by the strong *J*-aggregation of PY-IT.

This article is protected by copyright. All rights reserved.

15214095, ja, Downloaded from https://onlinelibrary.wiley.com/doi/10.1002/adma.202212275 by Hong Kong Poly University, Wiley Online Library on [10/02/2023]. See the Terms and Conditions (https://onlinelibrary.wiley.com/terms-and-conditions) on Wiley Online Library for rules of use; OA articles are governed by the applicable Creative Commons License

Accepted Article

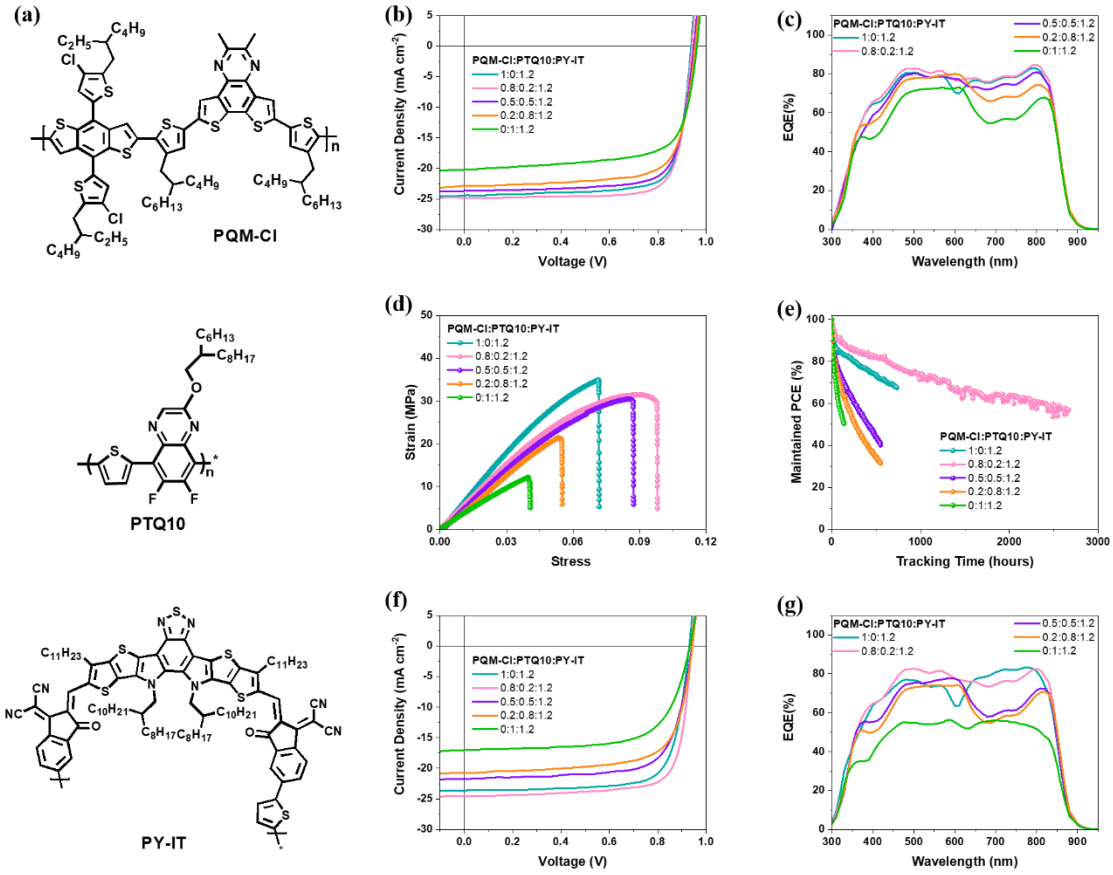

Figure 1. (a) Chemical structures of PQM-Cl, PTQ10, and PY-IT. (b) *J-V* characteristics and (c) the related EQE spectra of all-PSC devices. (d) The strain-stress curves of the blend films with different material ratios. (e) The MPP tracking results. (f) *J-V* characteristics and (g) the related EQE spectra of all-PSC devices based on 10-hour light-soaked burn-in films.

All-PSCs with a conventional device architecture of ITO/PEDOT:PSS/PQM-Cl:PTQ10:PY-IT/PFN-Br-MA[41]/Ag are fabricated to evaluated photovoltaic performance. The *J-V* characteristics and corresponding parameters are given in **Figure 1b** and **Table 1**, respectively. The binary PQM-Cl:PY-IT devices demonstrate a PCE of 17.78% with both excellent J_{SC} (24.17 mA cm^{-2}) and *FF* (77.6%). When introducing PTQ10 as the third component into PQM-Cl:PY-IT host system, the optimized ternary PQM-Cl:PTQ10:PY-IT (0.8:0.2:1.2) device demonstrates an impressive PCE of 18.45% due

This article is protected by copyright. All rights reserved.

15214095, ja, Downloaded from https://onlinelibrary.wiley.com/doi/10.1002/adma.202212275 by Hong Kong Poly University, Wiley Online Library on [10/02/2023]. See the Terms and Conditions (https://onlinelibrary.wiley.com/terms-and-conditions) on Wiley Online Library for rules of use; OA articles are governed by the applicable Creative Commons License

Accepted Article

to all the slightly increased V_{OC}, J_{SC}, and *FF*. With the continuous increase of PTQ10 content, the PCEs of devices based on PQM-Cl:PTQ10:PY-IT with different weight ratios gradually decrease to 17.06% for 0.5:0.5:1.2, then to 16.11% for 0.2:0.8:1.2 and 13.69% for 0:1:1.2. To find out charge generation change brought by PTQ10 introduction, and also to make sure the reliability of the device results, the external quantum efficiency (EQE) spectra are measured, as illustrated in **Figure 1c**. The integrated J_{SC} values indicate that measurement mismatches for all devices are less than 3%. The increasing EQE part of optimal ternary device compared with PQM-Cl-based binary one is located at 450-650 nm, which is supposed to be contributed by PTQ10. To explain this variation, further discussion will be provided later.

Table 1. Photovoltaic parameters for all-PSCs based on QM-Cl:PTQ10:PY-IT with different weight ratios.

PQM-Cl:PTQ10:PY-IT	V_{OC} (V)	J_{SC} (mA cm^{-2})[a]	*FF* (%)	PCE (%)[b]
Fresh				
1:0:1.2	0.938	24.17/23.54	77.6	17.78 (17.45±0.22)
0.8:0.2:1.2	0.943	24.80/24.16	78.9	18.45 (18.12±0.32)
0.5:0.5:1.2	0.950	23.69/23.08	75.8	17.06 (16.75±0.25)
0.2:0.8:1.2	0.955	22.86/22.33	73.8	16.11 (15.76±0.30)
0:1:1.2	0.962	20.21/19.80	70.4	13.69 (13.38±0.26)
Soaked				
1:0:1.2	0.931	23.63/23.08	76.0	16.72 (16.20±0.53)
0.8:0.2:1.2	0.939	24.56/23.80	77.3	17.85 (17.63±0.31)

This article is protected by copyright. All rights reserved.

15214095, ja, Downloaded from https://onlinelibrary.wiley.com/doi/10.1002/adma.202212275 by Hong Kong Poly University, Wiley Online Library on [10/02/2023]. See the Terms and Conditions (https://onlinelibrary.wiley.com/terms-and-conditions) on Wiley Online Library for rules of use; OA articles are governed by the applicable Creative Commons License

0.5:0.5:1.2	0.942	21.71/21.03	72.3	14.78 (14.06±0.61)
0.2:0.8:1.2	0.943	20.73/20.30	70.6	13.80 (13.27±0.42)
0:1:1.2	0.943	17.03/16.32	68.0	10.92 (10.48±0.39)

[a]EQE integrated J_{SC} values are listed after the slashes. [b]The brackets contain averages and standard errors of PCEs based on at least 20 devices.

Then crack-onset-strain (COS) as another important figure-of-merit for all-polymer blend is evaluated, which represents the film ductility.[42-47] As presented in **Figure 1d** and **Table S1**, the strain-stress curves of all-polymer blends are presented in Figure 2d and their derived COS and mechanical toughness values are listed in **Table S1**. It was found that the proper addition PTQ10 could significantly boost the ductility of active layers in this work. As for the underlying reason for the non-monotonic variation of film ductility along PTQ10 content in active layers, it shall be a complicated coherence of the chemical structure, molecular weight, crystallinity in film etc. of photovoltaic materials. Both boosted active layer ductility and improved efficiency synergistically strengthen the value of investigating the optimal ternary system's light soaking stability.

Accordingly, the operational stability of encapsulated all-PSCs with different blend ratios is detected under 1-sun white LED illumination with an automatic MPP tracking. Corresponding results are portrayed in **Figure 1e**, where the best stability is observed in 20 wt% PTQ10 possessed ternary device, which is clearly better than its biggest counterpart. Notably, the device parameters of the optimal system at 2000-hour tracking point are V_{OC} = 0.772 V, J_{SC} = 22.96 mA cm^{-2}, *FF* = 65.6 %, PCE = 11.63 %. As for other blend systems with much higher PTQ10 content (more than 50%), the stability becomes significantly poorer, implying PTQ10 is intrinsically instable in film morphologically. Concentrating on the advantage of optimal ternary device in stability, it mainly relies on the reduced burn-in

This article is protected by copyright. All rights reserved.

Accepted Article

15214095, ja, Downloaded from https://onlinelibrary.wiley.com/doi/10.1002/adma.202212275 by Hong Kong Poly University, Wiley Online Library on [10/02/2023]. See the Terms and Conditions (https://onlinelibrary.wiley.com/terms-and-conditions) on Wiley Online Library for rules of use; OA articles are governed by the applicable Creative Commons License

loss at the initial stage, for its slow degradation region is highly similar to that of PQM-Cl binary system. Thereafter, understanding the burn-in loss alleviation by addition PTQ10 with proper ratio is the essence of this work. Then "burn-in" devices are fabricated based on ITO/PEDOT:PSS/PQM-Cl:PTQ10:PY-IT samples that pre-soaked for 10 hours under 1-sun illumination in N_2-filled glovebox, followed by PFN-Br-MA spin coating and Ag electrode thermal evaporation. The related *J-V* characteristics and EQE spectra are showed in **Figure 1f** and **1g**, respectively, while their photovoltaic parameters are summarized in **Table 1**. It is consistent that the optimal ternary blend (0.8:0.2:1.2) shows the lowest PCE loss rate of 3.25%, while the PQM-Cl:PY-IT binary devices also has a relatively lower PCE decrease rate of 5.96% and the other systems with higher PTQ10 content suffer from great PCE sacrifice >13%. Through carefully comparing the losses of each photovoltaic parameters, ternary blend with 20 wt% PTQ10 is helpful in keeping the high J_{SC}, while the FF maintaining rates of host and target systems are almost the same. To clearly figure out the burn-in loss alleviation, both morphological and physical mechanisms, as well as the thermal stability of all-PSCs with different PTQ10 contents should be carefully investigated.

This article is protected by copyright. All rights reserved.

Accepted Article

15214095, ja, Downloaded from https://onlinelibrary.wiley.com/doi/10.1002/adma.202212275 by Hong Kong Poly University, Wiley Online Library on [10/02/2023]. See the Terms and Conditions (https://onlinelibrary.wiley.com/terms-and-conditions) on Wiley Online Library for rules of use; OA articles are governed by the applicable Creative Commons License

Accepted Article

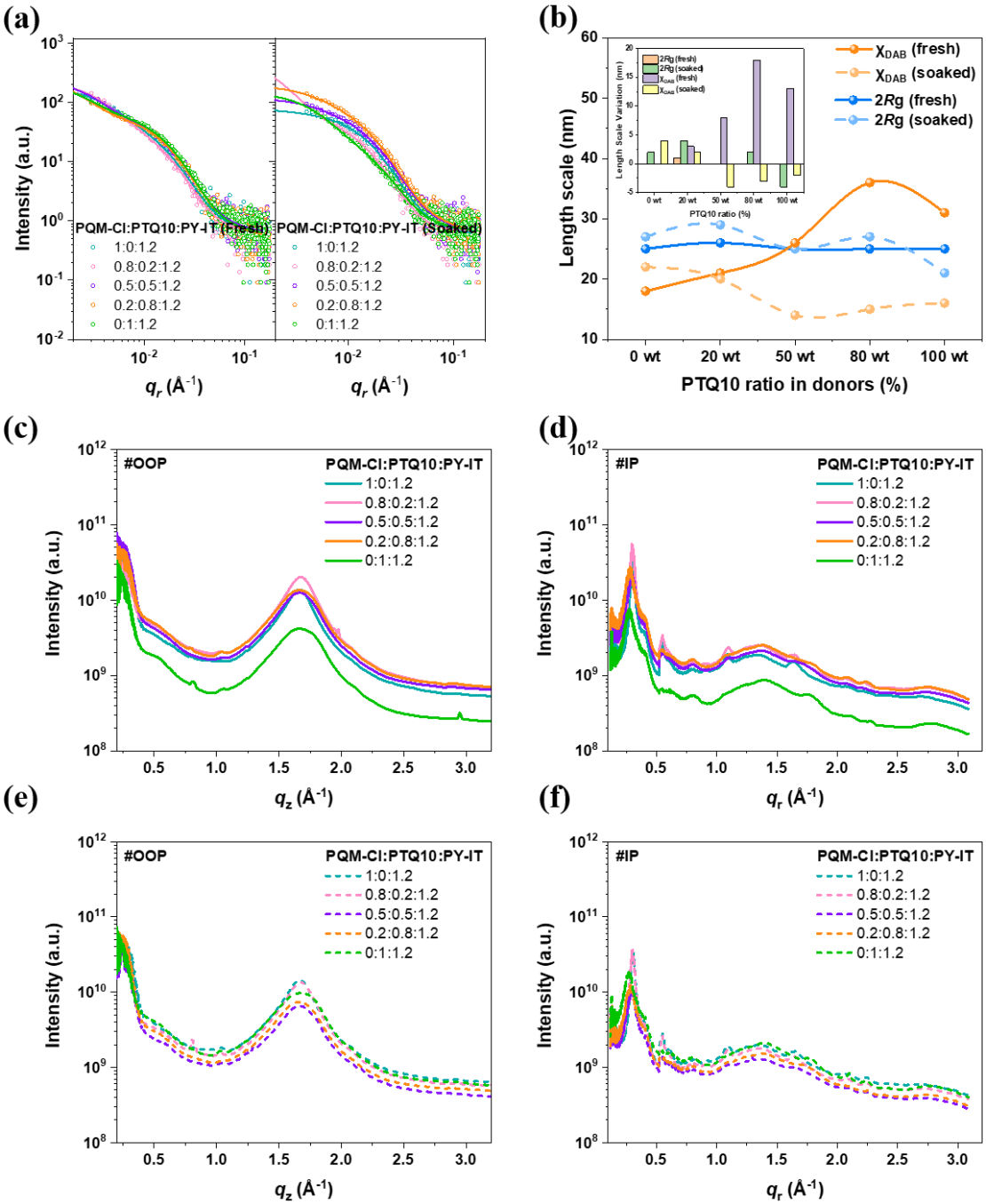

Figure 2. GISAXS IP intensity profiles of (a) fresh and soaked blend films. (b) The variation plots of derived phase separation length scales of fresh and soaked samples. Inserted graph is to demonstrate the length scale variation of other systems when setting up fresh PQM-Cl:PY-IT as the standard. For fresh blend films: (c) OOP line-cuts and (d) IP line-cuts. For "burn-in" degraded films: (g) OOP line-cuts and (h) IP line-cuts.

This article is protected by copyright. All rights reserved.

15214095, ja, Downloaded from https://onlinelibrary.wiley.com/doi/10.1002/adma.202212275 by Hong Kong Poly University, Wiley Online Library on [10/02/2023]. See the Terms and Conditions (https://onlinelibrary.wiley.com/terms-and-conditions) on Wiley Online Library for rules of use; OA articles are governed by the applicable Creative Commons License

Accepted Article

Then the morphology study begins with the atomic force spectroscopy (AFM) test, that can provide general information of film surface, and thus a glance of aggregation and possibly interpenetrating network of materials.[48] Based on the AFM height images given in **Figure S2a**, all fresh and soaked blend films with smooth surface show similar roughness of 1.20-1.76 nm no matter how the content of PTQ10 varies and whether the light soaking is applied, while no special interpretation can be persuasively offered. Therefore, more quantitative and smaller-scale analyses are carried out. The grazing incidence small angle X-ray scattering (GISAXS) measurements are utilized to have a description of phase separation behavior change.[49,50] The original patterns are given in **Figure S2b-c** and corresponding in-plane (IP) intensity profiles are plotted in **Figure 2a**. The fitting curves based on a reported model are also illustrated throughout the data plots.[51] Accordingly, length scales of pure acceptor phase ($2Rg$) and mixed phase (χ_{DAB}) are obtained and drawn as a variation plot along with PTQ10 content ratio for all fresh and soaked active layers in **Figure 2b**. The inserted figure is to reflect the variation of $2Rg$ and χ_{DAB} values of other blend films compared to fresh PQM-Cl:PY-IT binary host system. Empirically, the pure phase takes care of charge transport and the intermixing region is responsible for charge generation, so a balanced distribution and separation length scales are vital parameters to judge if the morphology is favorable to boosting device performance.[52] The $2Rg$ and χ_{DAB} values of fresh PQM-Cl:PY-IT film are 25 and 18 nm, respectively. Considering its excellent J_{SC} and *FF* values in device, this kind of phase separation can be taken as a standard. Therefore, the change of these values in optimal ternary system (fresh one) indicates a larger chance of charge generation, and concurrently better charge transport ($2Rg$ = 26 nm and χ_{DAB} = 21nm), which are consistent with promoted J_{SC} and FF values. For films with higher PTQ10 ratio, the $2Rg$ values are uniformly 25 nm, but the χ_{DAB} values are 26, 36, and 31 nm, with the increase of PTQ10's weight ratio. These results imply that the general self-aggregation

This article is protected by copyright. All rights reserved.

15214095, ja, Downloaded from https://onlinelibrary.wiley.com/doi/10.1002/adma.202212275 by Hong Kong Poly University, Wiley Online Library on [10/02/2023]. See the Terms and Conditions (https://onlinelibrary.wiley.com/terms-and-conditions) on Wiley Online Library for rules of use; OA articles are governed by the applicable Creative Commons License

Accepted Article

behavior of PY-IT is not affected by tuning the ratio of PMQ-Cl:PTQ10 donor materials, so the morphology determination is possibly dominated by PY-IT's crystallization induced phase separation. It is easy understandable from the point of film formation process, where main solvent CF evaporated soon, resulting in fast precipitation of PQM-Cl and PTQ10, while PY-IT that is well miscible in 1-chloronaphthalene (1-CN) could take a longer drying time for crystal growth.[51] Here it also demonstrated that the oversized mixed region could be detrimental to J_{SC}, as argued by previous works.[54-55] As for the soaked samples, low PTQ10 ratio contained ones exhibit limited variation for two type length scales, coinciding with their better device performances after "burn-in" light stress. The optimal ternary film shows almost no change in intermixing phase size, which could be the reason of its better J_{SC} maintaining rate than PQM-Cl:PY-IT. Furthermore, the size of intermixing phase goes to a very low level for all high PTQ10 weight ratio blends. It seems such strict loss is also detrimental to J_{SC} values. Interestingly, we prove again that intermixing phase length scale is not wanted to be too large or too small. Besides, the pure acceptor phase's size is fluctuating in different systems, suggesting PY-IT's phase is stable. The χ_{DAB} variation tendency exhibited by PTQ10:PY-IT is opposite to that of PQM-Cl (shrinking *vs* swelling), which might reach a balance in 20 wt% PTQ10 contained system, and thus well-kept χ_{DAB}.

Moreover, grazing incidence wide angle X-ray scattering (GIWAXS) technology is used for probe molecular packing, crystallinity and thus charge transport.[56] The 2D patterns of fresh and soaked active layers are presented in **Figure S2d**, from which extracted IP and out-of-plane (OOP) directional line-cuts are displayed in **Figure 2c-f**. Corresponding fitted parameters including peak position, *d*-spacing, and coherence length (CL) values are summarized in **Table S2-3**. Combining with UV-vis absorption profile, the transition from *J*-aggregation to *H*-aggregation dominance of donor polymer(s) by blending them with PY-IT is the result of the strong IP (100) diffraction peak signals for all blend films. Thereby, the evaluation of CL variation of lamellar peak is an effective way to predict the hole transport

This article is protected by copyright. All rights reserved.

15214095, ja, Downloaded from https://onlinelibrary.wiley.com/doi/10.1002/adma.202212275 by Hong Kong Poly University, Wiley Online Library on [10/02/2023]. See the Terms and Conditions (https://onlinelibrary.wiley.com/terms-and-conditions) on Wiley Online Library for rules of use; OA articles are governed by the applicable Creative Commons License

Accepted Article

change in different blend systems combined by the intrinsic hole mobility (μ_h) of PQM-Cl and PTQ10. The "burn-in" light stress results in negligible CL value variation, thereby hole transport variation shall be minor. The electron transport/mobility (μ_e) change can be explained by GISAXS calculated phase length scale and the CL of π-π stacking peak by GIWAXS. The *d*-spacing and CL values of blend films before and after light soaking differ insignificantly, and the phase separation length scales are also stable, so the electron transport contributed by PY-IT pure domain is supposed to lie on a similar level, too. In view of this, a series of hole-only and electron-only devices are fabricated to obtain the mobilities according to space charge limited current (SCLC) method. The *J-V* curves of all type devices are illustrated in **Figure S3a-c**, and the results (μ_h, μ_e and μ_h/μ_e) are listed in **Table S4**. The hypothesis based on GIWAXS analysis is mostly supported, except for PTQ10:PY-IT binary film, which shows significant reduction of hole transport ability after "burn-in" illumination. In a horizontal comparison, three polymer materials have high mobilities, but PTQ10-rich blend films exhibit lower μ_h and μ_e values. These results indicate that PTQ10 in active layer is strongly suppressed by PY-IT during its crystallization, thereby poor hole transporting ability for lack of high-quality crystallites. As for optimal ternary system, 20 wt% PTQ10 can be well distributed over PQM-Cl's crystalline phase, and efficiently assist the hole transporting. Therefore, the efficiency degradation of PTQ10-based binary solar cells can be partially (mainly the *FF*) explained by μ_h loss, but the change of other systems, especially the J_{SC} loss cannot be well understood. This analysis also endorses the non-monotonic COS value variation observed before. PTQ10 has been previously found sensitive to solvent additive treatment and thermal annealing in terms of crystallinity and film ductility.[57] Posttreatment free PTQ10 is highly stretchable, while treated counterpart exhibits much poorer performance, which might be attributed to its simple structure. Herein, when PTQ10 takes great proportion in blend (50% or more), the film ductility will of course be reduced since 2 vol% 1-CN and 100 ℃ annealing. For 20 wt% incorporation case, the solvent additive and annealing mainly affect PQM-Cl related crystallites, so PTQ10 could bear a chance of

This article is protected by copyright. All rights reserved.

15214095, ja, Downloaded from https://onlinelibrary.wiley.com/doi/10.1002/adma.202212275 by Hong Kong Poly University, Wiley Online Library on [10/02/2023]. See the Terms and Conditions (https://onlinelibrary.wiley.com/terms-and-conditions) on Wiley Online Library for rules of use; OA articles are governed by the applicable Creative Commons License

Accepted Article

playing as a ductility enhancer since low posttreatment stress is applied on it. To further figure out the degradation mechanism and the improvement of fresh device efficiencies, more attentions should be paid on charge transfer. Subsequently, correlating the charge transfer and transport can make a clearer description for generation and recombination dynamics.

Before that, some basic characterizations are implemented for a general information of device physics. **Figure S3d** depicts the photocurrent *versus* effective voltage (J_{ph} *vs* V_{eff}) curves of fresh devices, with deduced saturated current density, charge dissociation probability and charge collection efficiency (J_{sat}, η_{diss}, η_{coll}) values in **Table S5**. It shows that all systems contain very efficient charge dissociation, so geminate recombination contributes negligibly to monomolecular recombination. Fitting from **Figure S3e**, the ideal factors are 1.12, 1.02, 1.16, 1.25, and 1.26 for the all-PSCs with the increase of PTQ10 content.[58] Meanwhile extracting from J_{SC} *vs* light intensity curves in **Figure S3f**, the *S* values are 0.976, 0.977, 0.976, 0.972, and 0.971.[59] Obviously, bimolecular recombination varies insignificantly as well. Then we can claim reduced trap-assisted recombination leads to promoted FF in optimal ternary device.

This article is protected by copyright. All rights reserved.

15214095, ja, Downloaded from https://onlinelibrary.wiley.com/doi/10.1002/adma.202212275 by Hong Kong Poly University, Wiley Online Library on [10/02/2023]. See the Terms and Conditions (https://onlinelibrary.wiley.com/terms-and-conditions) on Wiley Online Library for rules of use; OA articles are governed by the applicable Creative Commons License

Accepted Article

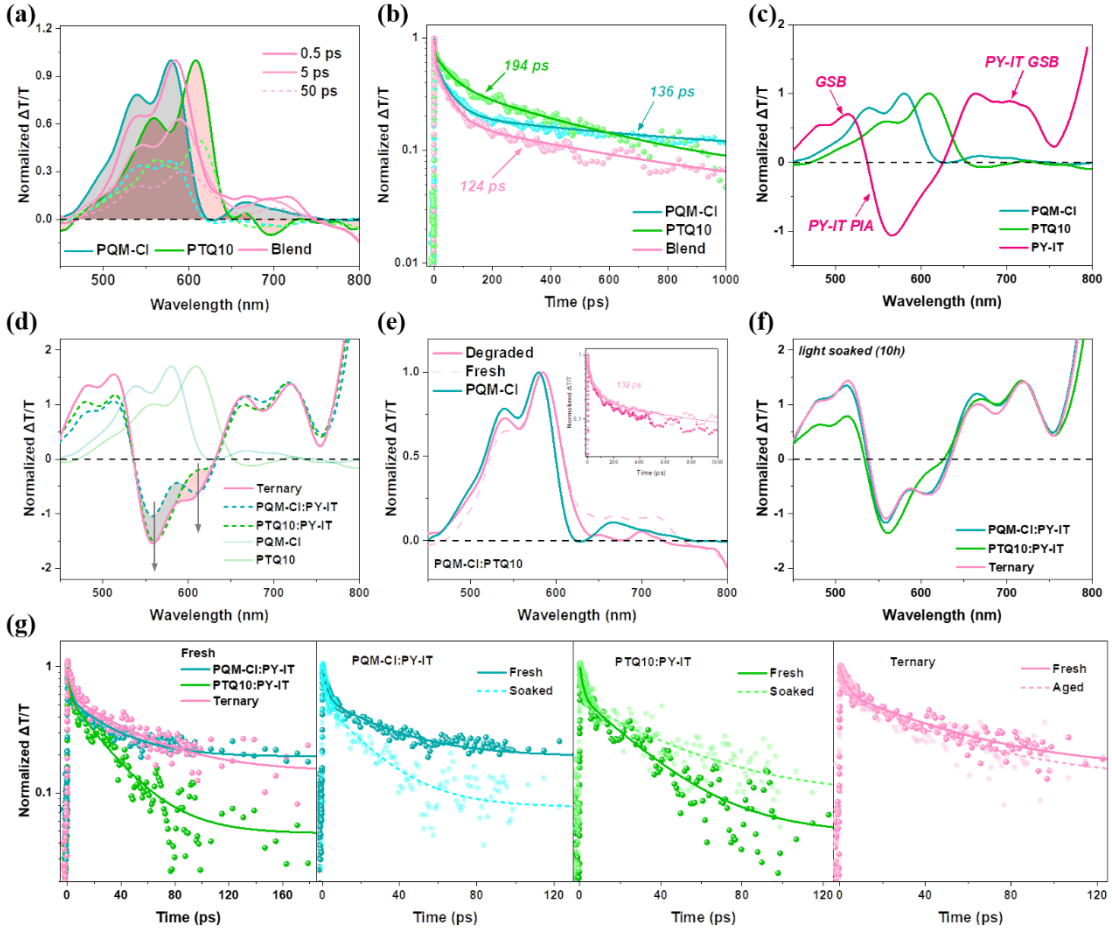

Figure 3. fs-TAS spectra presented in term of ΔT/T: (a) Donor films spectral line cuts at representative time. (b) Donor films GSB decay kinetics fitting. (c) TAS profile comparison of PQM-Cl, PTQ10, and PY-IT neat films. (d) TAS profile comparison of binary/ternary films and neat donor films. (e) The "burn in" light soaking effect on PQM-Cl:PTQ10 blend films and decay kinetics. (f) TAS profile comparison of degraded binary & ternary films. (g) Decay kinetics analyses on binary/ternary films in fresh and soaked statuses.

Turning back to the main line, the femtosecond resolved transient absorption spectra (fs-TAS) for neat films, fresh and soaked donor blend films, fresh and soaked donor-acceptor blend films are demonstrated. Beginning from studies of the donor polymer films, the PQM-Cl and PTQ10 based neat and blend films are excited by a 400 nm pump laser wherein

This article is protected by copyright. All rights reserved.

15214095, ja, Downloaded from https://onlinelibrary.wiley.com/doi/10.1002/adma.202212275 by Hong Kong Poly University, Wiley Online Library on [10/02/2023]. See the Terms and Conditions (https://onlinelibrary.wiley.com/terms-and-conditions) on Wiley Online Library for rules of use; OA articles are governed by the applicable Creative Commons License

Accepted Article

their ground state bleach (GSB) signals are observed with good match to absorption spectra. Spectral line cuts at various delay times are illustrated in **Figure 3a**, from which one can see the GSB features of blend films in between those from pure films, suggesting both donor materials absorbing light efficiently in blend. 50 ps after excitation, the GSB signals are largely quenched, owing to S_1-S_0 recombination, while the blend film exhibits the fastest decay. This phenomenon can be assigned to charge transfer and additional generation at the PQM-Cl/PTQ10 phase interface, and it could be related to boosted J_{SC} and FF in optimal ternary device. The singlet exciton GSB decay analysis in **Figure 3b** further supports above discussion, i.e.: 136, 194, and 124 ps are the calculated lifetime for PQM-Cl and PTQ10 neat film and related blend films, respectively. Here the lifetime is equal to the weighted average values of sum of multi-exponential fitting. Next, we put the PY-IT's signal excited at 800 nm together with two donor pure films in **Figure 3c**, and the related normalized spectra of fresh binary/ternary blend films are shown in **Figure 3d**. These cuts are all extracted at 0.5 ps. Thus, the characteristic coupling of two binary systems was observed in the photo-induced absorption (PIA) of ternary blends. In binary/ternary films, PIA signals observed of PY-IT is influenced by the positive hole polaron GSB upon charge transfer from PY-IT: the PIA at 530-600 nm region is reduced in PQM-Cl:PY-IT fresh film due to the hole polarons of PQM-Cl; likewise, PIA at 600-640 nm is weakened by PTQ10's hole polaron in PTQ10:PY-IT. Hence, there should be multi-pathways for charge generation *via* hole transfer that can occur at interface of PY-IT to either of the donors. This is going to enhance charge generation as evident by the increased hole polarons GSB at 450-530 nm. Upcoming active layer signal decay analysis is enabled by presenting their profile at specific time in **Figure S4**. The hole polaron GSB surpasses the PY-IT's remained singlet PIA, leading to positive peak within 560-630 nm for binary and ternary blend films. Notably, only PQM-Cl's hole polaron GSB feature remains even after 7 ns for optimal ternary film, bringing a hypothesis that hole polarons tend transporting to PQM-Cl prior to extraction. Nevertheless, the

This article is protected by copyright. All rights reserved.

15214095, ja, Downloaded from https://onlinelibrary.wiley.com/doi/10.1002/adma.202212275 by Hong Kong Poly University, Wiley Online Library on [10/02/2023]. See the Terms and Conditions (https://onlinelibrary.wiley.com/terms-and-conditions) on Wiley Online Library for rules of use; OA articles are governed by the applicable Creative Commons License

Accepted Article

additional charge transfer pathway observed between PQM-Cl and PTQ10 is believed to reduce the chance of nongeminate recombination.

As for stability mechanism exploitation, the donor-blend film (PQM-Cl:PTQ10) is firstly investigated, as presented in **Figure 3e**. The 10-hour illuminated blend film's initial singlet (0.5ps) GSB resembles more the PQM-Cl. Parallelly, its decay time becomes slower (124 ps to 132 ps) and closer to that of PQM-Cl (136 ps). The fitting process is drawn and inserted in **Figure 3e**, and the corresponding fitting details are summarized in **Table S6**. Meanwhile, **Figure 3f** presents the initial TAS profile (0.5 ps) of degraded binary and ternary active layers. The phenomenon of ternary film's profile turns to be more like PQM-Cl:PY-IT binary system, which is coincides with the above discovery. Therefore, the charge generation of PTQ10:PY-IT blend is sought to be substantially reduced after light soaking compared with the fresh one as indicated by the downshift GSB features in 450-530 nm. In other words, PTQ10 is relatively unstable, consistent with morphology analysis. The charge generation after light soaking prefers to migrate to what is held by PQM-Cl:PY-IT system, which is also efficient. Though PTQ10 in ternary film seems unstable, but co-existed PQM-Cl turns to be stabler. Hence, "burn-in" active layer based optimal ternary device exhibits the photovoltaic performance nearly identical to that of fresh PQM-Cl:PY-IT system. Furthermore, the spectra enabled analysis is strengthened by hole transfer kinetics fitting results of active layers, as visualized in **Figure 3g**, and summarized in **Table S7**. For accurate analysis, low-fluence excitation (< 3 μJ cm^{-2}) is used to avoid interference from exciton-exciton annihilation (EEA). The calculated decay lifetime for the fresh devices based on binary PQM-Cl:PY-IT and PTQ10:PY-IT and their ternary systems are 16.6 ps, 15.6 ps, and 25.5 ps, respectively; while these values for degraded film-based devices are 10.9 ps, 21.0 ps, and 24.3 ps. It is obvious that ternary blend contains the slowest hole transfer, yet the best J_{SC} and *FF*. This phenomenon has already been argued by peers that slower rates may not destroy the generation efficiency.[60] The rate in essence reflects the energy landscape of material systems,

This article is protected by copyright. All rights reserved.

15214095, ja, Downloaded from https://onlinelibrary.wiley.com/doi/10.1002/adma.202212275 by Hong Kong Poly University, Wiley Online Library on [10/02/2023]. See the Terms and Conditions (https://onlinelibrary.wiley.com/terms-and-conditions) on Wiley Online Library for rules of use; OA articles are governed by the applicable Creative Commons License

Accepted Article

and in some cases slower hole transfer might even improve the charge generation. Furthermore, lower hole transfer could approach a balance between charge generation and transport if the hole transport is not so fast, and thus possibly improving the FF of devices. On the other hand, the fastest hole transfer of PTQ10 might be enabled by its large intermixing domain size as demonstrated by GISAXS experiments. For “burn-in” films, very marginal variation takes place for ternary blend, reflecting its good stability. The opposite hole transfer speed evolution direction of PQM-Cl:PY-IT and PTQ10:PY-IT (slowing down *vs* accelerating) is consistent with their morphology evolution tendency, and further support the stable hole transfer rate of ternary film before and after 10-hour light soaking (the cancelling-out effect).

This article is protected by copyright. All rights reserved.

15214095, ja, Downloaded from https://onlinelibrary.wiley.com/doi/10.1002/adma.202212275 by Hong Kong Poly University, Wiley Online Library on [10/02/2023]. See the Terms and Conditions (https://onlinelibrary.wiley.com/terms-and-conditions) on Wiley Online Library for rules of use; OA articles are governed by the applicable Creative Commons License

Accepted Article

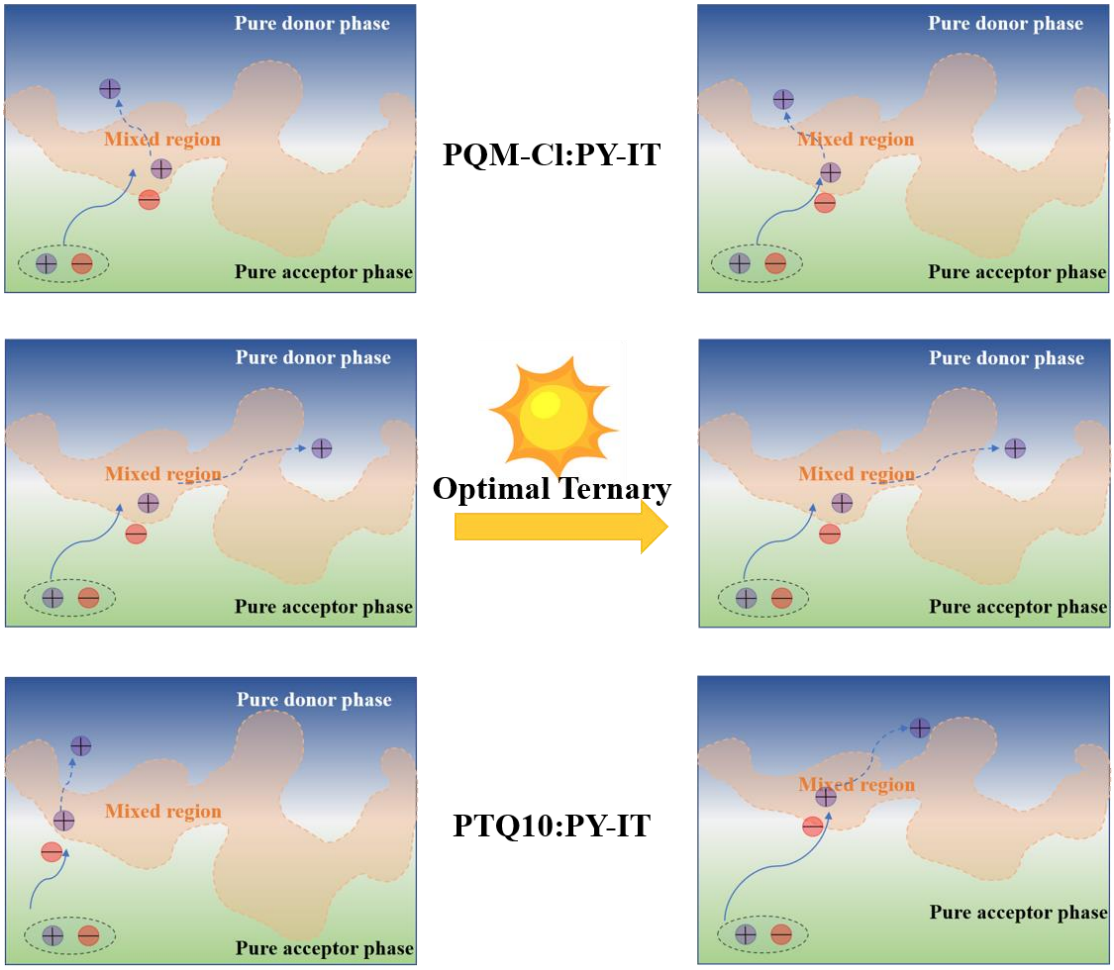

Figure 4. Schematic diagram of morphology evolution and exciton behaviors in binary and ternary systems.

For a comprehensive illustration of this ternary design's effect in device performance degradation alleviation, the schematic diagram of morphology evolution and exciton behaviors in active layers was presented in **Figure 4** herein. As for the PQM-Cl:PY-IT control system, its fresh film demonstrates a suitable phase separation feature for charge generation and transport, and charge transfer (this work only focus on hole transfer because electron transfer is widely acknowledged very efficient) takes place in a medium speed through the intermixing phase. PTQ10:PY-IT morphology contains a large mixed region,

This article is protected by copyright. All rights reserved.

15214095, ja, Downloaded from https://onlinelibrary.wiley.com/doi/10.1002/adma.202212275 by Hong Kong Poly University, Wiley Online Library on [10/02/2023]. See the Terms and Conditions (https://onlinelibrary.wiley.com/terms-and-conditions) on Wiley Online Library for rules of use; OA articles are governed by the applicable Creative Commons License

Accepted Article

thus pure donor phase in some places is closer to pure acceptor phase, which is able to result in faster hole transfer kinetics for fresh sample. Driven by "burn-in" light soaking, PQM-Cl composed binary film shows an enlarged χ_{DAB}, thus generally faster hole transfer rate. Meanwhile, PTQ10:PY-IT's big-size intermixing domain shrinks a lot, which makes longer diffusion distance for excitons to go, thereby high possibility of slower hole transfer. In the fresh optimal ternary system, morphological feature is very similar to that of PQM-Cl:PY-IT, but much slower hole transfer speed is demonstrated, implying the introduction of PTQ10 changes the hole transfer pathway. Since the charge transport/mobility of photovoltaic materials is normally moderate, slower transfer rate could contribute to reducing non-geminate recombination, thereby promoted *FF*. Furthermore, the ternary film maintains the general morphology characteristics after 1-sun treatment for 10 hours, thanks to the counteract of degradation directions of PQM-Cl and PTQ10 based binary systems. Thus, its exciton behavior is also well kept.

Furthermore, the "cancelling out" strategy in this work could play greater role in the future, not limited in the field of all-PSC, but the whole OPV field. An effective material selection for typical ternary matrix should be based on the full knowledge upon binary host systems. With a pre-experimental investigation upon film morphology degradation where counteract evolutions of phase length scale will possibly endorse the success of "cancelling out" method. This shall not be only applicable for ternary systems with two donors and one acceptor, but also those of one donor and two acceptors, for which some former works imply similar concepts.[61] To predict the morphology evolution direction without tremendous experimental input, one can refer to thermodynamical and kinetical analysis upon crystallization and phase separation.[62]

This article is protected by copyright. All rights reserved.

15214095, ja, Downloaded from https://onlinelibrary.wiley.com/doi/10.1002/adma.202212275 by Hong Kong Poly University, Wiley Online Library on [10/02/2023]. See the Terms and Conditions (https://onlinelibrary.wiley.com/terms-and-conditions) on Wiley Online Library for rules of use; OA articles are governed by the applicable Creative Commons License

Accepted Article

Conclusion

In summary, we hereby focus on the most concerned topic of all-PSCs, such as ternary device design, the photo-stability and underlying mechanism. Compared to the binary all-PSCs based on PQM-Cl:PY-IT and PTQ10:PY-IT, the PQM-Cl:PTQ10:PY-IT (0.8:0.2:1.2)-based ternary all-PSCs achieved simultaneously improved PCE, film ductility, and device stability. The device lifetime elongation is enabled by burn-in loss alleviation, so further understanding works are done by comparing fresh films and photo-degraded ones, in term of PCEs, morphological features, and exciton behaviors. It is then found that PQM-Cl and PTQ10 exhibit opposite morphological evolution tendency and fortunately reach a balance when blending them, resulting in a well-maintained phase length scale for the pure and mixed. These kind of cancelling out strategy succeeds in keeping charge transfer kinetics, as well. Therefore, this work reveals the underlying physical and morphological mechanism for delicate ternary blend design enabled “burn-in” loss reduction for efficient and stable all-PSCs.

Conflict of Interest

Authors declare no conflict of interest.

Supporting Information

Supporting Information is available from the Wiley Online Library or from the author.

Data Availability

This article is protected by copyright. All rights reserved.

15214095, ja, Downloaded from https://onlinelibrary.wiley.com/doi/10.1002/adma.202212275 by Hong Kong Poly University, Wiley Online Library on [10/02/2023]. See the Terms and Conditions (https://onlinelibrary.wiley.com/terms-and-conditions) on Wiley Online Library for rules of use; OA articles are governed by the applicable Creative Commons License

Accepted Article

The data that support the findings of this study are available from the corresponding authors on reasonable request.

Acknowledgements

G. Li acknowledges the support from Research Grants Council of Hong Kong (Project Nos 15320216, 15221320, C5037-18G), RGC Senior Research Fellowship Scheme (SRFS2122-5S04), National Natural Science Foundation of China (51961165102), Shenzhen Science and Technology Innovation Commission (JCYJ20200109105003940, SGDX2019081623220944), the Hong Kong Polytechnic University Internal Research Funds: Sir Sze-yuen Chung Endowed Professorship Fund (8-8480), RISE (1-CDA5), 1-W15V, and Guangdong-Hong Kong-Macao Joint Laboratory for Photonic-Thermal-Electrical Energy Materials and Devices (GDSTC No. 2019B121205001). W. Ma and Q. Fan thank the support from National Natural Science Foundation of China (21704082, 21875182, 22209131), Key Scientific and Technological Innovation Team Project of Shaanxi Province (2020TD-002), 111 project 2.0 (BP2018008). R. Ma thanks the support by PolyU Distinguished Postdoc Fellowship. X-ray data was acquired at beamlines 7.3.3 and 11.0.1.2 at the Advanced Light Source, which is supported by the Director, Office of Science, Office of Basic Energy Sciences, of the U.S. Department of Energy under Contract No. DE-AC02-05CH11231. The authors thank Dr. Eric Schaible and Dr. Chenhui Zhu at beamline 7.3.3, and Dr. Cheng Wang at beamline 11.0.1.2 for assistance with data acquisition. Prof. Jianhui Hou and his team are appreciated for PQM-Cl.

This article is protected by copyright. All rights reserved.

15214095, ja, Downloaded from https://onlinelibrary.wiley.com/doi/10.1002/adma.202212275 by Hong Kong Poly University, Wiley Online Library on [10/02/2023]. See the Terms and Conditions (https://onlinelibrary.wiley.com/terms-and-conditions) on Wiley Online Library for rules of use; OA articles are governed by the applicable Creative Commons License

Accepted Article

Author Contribution

Ruijie Ma: Conceptualization, Investigation, Formal Analysis, Methodology, Writing – Original Draft, Writing – Review & Editing, Project Administration

Qunping Fan: Resources, Writing – Review & Editing, Project Administration

Top Archie Dela Peña: Investigation, Formal Analysis, Writing – Original Draft

Baohua Wu: Investigation, Formal Analysis

Heng Liu: Investigation, Formal Analysis

Qiang Wu: Investigation

Qi Wei: Investigation

Jiaying Wu: Resources

Xinhui Lu: Resources

Mingjie Li: Resources

Wei Ma: Resources, Funding Acquisition, Supervision

Gang Li: Resources, Funding Acquisition, Supervision

Reference

1. C. Lee, S. Lee, G.-U. Kim, W. Lee, B. J. Kim, *Chem. Rev.* **2019**, 119, 8028.

2. G. Wang, F. S. Melkonyan, A. Facchetti, T. J. Marks, *Angew. Chem. Int. Ed.* **2019**, 58, 4129.

3. C. R. McNeill, *Energy Environ. Sci.* **2012**, 5, 5653.

This article is protected by copyright. All rights reserved.

15214095, ja, Downloaded from https://onlinelibrary.wiley.com/doi/10.1002/adma.202212275 by Hong Kong Poly University, Wiley Online Library on [10/02/2023]. See the Terms and Conditions (https://onlinelibrary.wiley.com/terms-and-conditions) on Wiley Online Library for rules of use; OA articles are governed by the applicable Creative Commons License

Accepted Article

4. J.-W. Lee, C. Sun, B. S. Ma, H. J. Kim, C. Wang, J. M. Ryu, C. Lim, T.-S. Kim, Y.-H. Kim, S.-K. Kwon, B. J. Kim, *Adv. Energy Mater.* **2021**, 11, 2003367.

5. Y. Xu, J. Yuan, S. Zhou, M. Seifrid, L. Ying, B. Li, F. Huang, G. C. Bazan, W. Ma, *Adv. Funct. Mater.* **2019**, 29, 1806747.

6. Z.-G. Zhang, Y. Yang, J. Yao, L. Xue, S. Chen, X. Li, W. Morrison, C. Yang, Y. Li, *Angew. Chem. Int. Ed.* **2017**, 56, 13503.

7. K. Zhou, K. Xian, L. Ye, *InfoMat* **2022**, 4, e12270.

8. Y. Kong, Y. Li, J. Yuan, L. Ding, *InfoMat* **2022**, 4, e12271.

9. Z.-G. Zhang, Y. Li, *Angew. Chem. Int. Ed.* **2021**, 60, 4422.

10. C. Duan, L. Ding, *Sci. Bull.* **2020**, 65, 1508.

11. D. Zhou, C. Liao, S. Peng, X. Xu, Y. Guo, J. Xia, H. Meng, L. Yu, R. Li, Q. Peng, *Adv. Sci.* **2022**, 9, 2202022.

12. J. Zhang, Q. Huang, K. Zhang, T. Jia, J. Jing, Y. Chen, Y. Li, Y. Chen, X. Lu, H. Wu, F. Huang, Y. Cao, *Energy Environ. Sci.* **2022**, DOI: 10.1039/D2EE01996E.

13. Q. Fan, R. Ma, W. Su, Q. Zhu, Z. Luo, K. Chen, Y. Tang, F. R. Lin, Y. Li, H. Yan, C. Yang, A. K. Y. Jen, W. Ma, *Carbon Energy* **2022**, DOI: 10.1002/cey2.267.

14. K. Hu, C. Zhu, K. Ding, S. Qin, W. Lai, J. Du, J. Zhang, Z. Wei, X. Li, Z. Zhang, L. Meng, H. Ade, Y. Li, *Energy Environ. Sci.* **2022**, 15, 4157.

15. J. Song, Y. Li, Y. Cai, R. Zhang, S. Wang, J. Xin, L. Han, D. Wei, W. Ma, F. Gao, Y. Sun, *Matter* **2022**, 5, 4047.

16. Y. Yue, B. Zheng, J. Ni, W. Yang, L. Huo, J. Wang, L. Jiang, *Adv. Sci.* **2022**, n/a, 2204030.

17. L. Zhu, M. Zhang, J. Xu, C. Li, J. Yan, G. Zhou, W. Zhong, T. Hao, J. Song, X. Xue, Z. Zhou, R. Zeng, H. Zhu, C.-C. Chen, R. C. I. MacKenzie, Y. Zou, J. Nelson, Y. Zhang, Y. Sun, F. Liu, *Nat. Mater.* **2022**, 21, 656.

18. R. Ma, C. Yan, J. Yu, T. Liu, H. Liu, Y. Li, J. Chen, Z. Luo, B. Tang, X. Lu, G. Li, H. Yan, *ACS Energy Lett.* **2022**, 7, 2547.

This article is protected by copyright. All rights reserved.

15214095, ja, Downloaded from https://onlinelibrary.wiley.com/doi/10.1002/adma.202212275 by Hong Kong Poly University, Wiley Online Library on [10/02/2023]. See the Terms and Conditions (https://onlinelibrary.wiley.com/terms-and-conditions) on Wiley Online Library for rules of use; OA articles are governed by the applicable Creative Commons License

Accepted Article

19. Y. Cui, Y. Xu, H. Yao, P. Bi, L. Hong, J. Zhang, Y. Zu, T. Zhang, J. Qin, J. Ren, Z. Chen, C. He, X. Hao, Z. Wei, J. Hou, *Adv. Mater.* **2021**, 33, 2102420.

20. Z. Luo, Y. Gao, H. Lai, Y. Li, Z. Wu, Z. Chen, R. Sun, J. Ren, C. e. Zhang, F. He, H. Woo, J. Min, C. Yang, *Energy Environ. Sci.* **2022**, 15, 4601.

21. Y. Wei, Z. Chen, G. Lu, N. Yu, C. Li, J. Gao, X. Gu, X. Hao, G. Lu, Z. Tang, J. Zhang, Z. Wei, X. Zhang, H. Huang, *Adv. Mater.* **2022**, 34, 2204718.

22. T. Liu, T. Yang, R. Ma, L. Zhan, Z. Luo, G. Zhang, Y. Li, K. Gao, Y. Xiao, J. Yu, X. Zou, H. Sun, M. Zhang, T. A. Dela Peña, Z. Xing, H. Liu, X. Li, G. Li, J. Huang, C. Duan, K. S. Wong, X. Lu, X. Guo, F. Gao, H. Chen, F. Huang, Y. Li, Y. Li, Y. Cao, B. Tang, H. Yan, *Joule* **2021**, 5, 914.

23. X. Yang, R. Sun, Y. Wang, M. Chen, X. Xia, X. Lu, G. Lu, J. Min, *Adv. Mater.* **2022**, n/a, 2209350.

24. T. Liu, K. Zhou, R. Ma, L. Zhang, C. Huang, Z. Luo, H. Zhu, S. Yao, C. Yang, B. Zou, L. Ye, *Aggregate* **2022**, n/a, e308.

25. R. Ma, J. Yu, T. Liu, G. Zhang, Y. Xiao, Z. Luo, G. Chai, Y. Chen, Q. Fan, W. Su, G. Li, E. Wang, X. Lu, F. Gao, B. Tang, H. Yan, *Aggregate* **2022**, 3, e58.

26. H. Sun, B. Liu, Y. Ma, J.-W. Lee, J. Yang, J. Wang, Y. Li, B. Li, K. Feng, Y. Shi, B. Zhang, D. Han, H. Meng, L. Niu, B. J. Kim, Q. Zheng, X. Guo, *Adv. Mater.* **2021**, 33, 2102635.

27. K. An, F. Peng, W. Zhong, W. Deng, D. Zhang, L. Ying, H. Wu, F. Huang, Y. Cao, *Sci. China Chem.* **2021**, 64, 2010.

28. R. Ma, K. Zhou, Y. Sun, T. Liu, Y. Kan, Y. Xiao, T. A. Dela Peña, Y. Li, X. Zou, Z. Xing, Z. Luo, K. S. Wong, X. Lu, L. Ye, H. Yan, K. Gao, *Matter* **2022**, 5, 725.

29. Q. Zhu, J. Xue, L. Zhang, J. Wen, B. Lin, H. B. Naveed, Z. Bi, J. Xin, H. Zhao, C. Zhao, K. Zhou, S. Liu, W. Ma, *Small* **2021**, 17, 2007011.

30. K. Zhou, K. Xian, Q. Qi, M. Gao, Z. Peng, J. Liu, Y. Liu, S. Li, Y. Zhang, Y. Geng, L. Ye, *Adv. Funct. Mater.* **2022**, 32, 2201781.

31. Y. Liang, D. Zhang, Z. Wu, T. Jia, L. Lüer, H. Tang, L. Hong, J. Zhang, K. Zhang, C. J. Brabec, N. Li, F. Huang, *Nat. Energy* **2022**, DOI: 10.1038/s41560-022-01155-x.

This article is protected by copyright. All rights reserved.

15214095, ja, Downloaded from https://onlinelibrary.wiley.com/doi/10.1002/adma.202212275 by Hong Kong Poly University, Wiley Online Library on [10/02/2023]. See the Terms and Conditions (https://onlinelibrary.wiley.com/terms-and-conditions) on Wiley Online Library for rules of use; OA articles are governed by the applicable Creative Commons License

Accepted Article

32. H. Cha, J. Wu, A. Wadsworth, J. Nagitta, S. Limbu, S. Pont, Z. Li, J. Searle, M. F. Wyatt, D. Baran, J.-S. Kim, I. McCulloch, J. R. Durrant, *Adv. Mater.* **2017**, 29, 1701156.

33. N. Gasparini, M. Salvador, S. Strohm, T. Heumueller, I. Levchuk, A. Wadsworth, J. H. Bannock, J. C. de Mello, H.-J. Egelhaaf, D. Baran, I. McCulloch, C. J. Brabec, *Adv. Energy Mater.* **2017**, 7, 1700770.

34. T. Heumueller, T. M. Burke, W. R. Mateker, I. T. Sachs-Quintana, K. Vandewal, C. J. Brabec, M. D. McGehee, *Adv. Energy Mater.* **2015**, 5, 1500111.

35. T. Heumueller, W. R. Mateker, I. T. Sachs-Quintana, K. Vandewal, J. A. Bartelt, T. M. Burke, T. Ameri, C. J. Brabec, M. D. McGehee, *Energy Environ. Sci.* **2014**, 7, 2974.

36. N. Li, J. D. Perea, T. Kassar, M. Richter, T. Heumueller, G. J. Matt, Y. Hou, N. S. Güldal, H. Chen, S. Chen, S. Langner, M. Berlinghof, T. Unruh, C. J. Brabec, *Nat. Commun.* **2017**, 8, 14541.

37. Z. Luo, T. Liu, R. Ma, Y. Xiao, L. Zhan, G. Zhang, H. Sun, F. Ni, G. Chai, J. Wang, C. Zhong, Y. Zou, X. Guo, X. Lu, H. Chen, H. Yan, C. Yang, *Adv. Mater.* **2020**, 32, 2005942.

38. J. Wang, Y. Cui, Y. Xu, K. Xian, P. Bi, Z. Chen, K. Zhou, L. Ma, T. Zhang, Y. Yang, Y. Zu, H. Yao, X. Hao, L. Ye, J. Hou, *Adv. Mater.* **2022**, 34, 2205009.

39. C. Sun, F. Pan, H. Bin, J. Zhang, L. Xue, B. Qiu, Z. Wei, Z.-G. Zhang, Y. Li, *Nat. Commun.* **2018**, 9, 743.

40. W. Zhang, C. Sun, I. Angunawela, L. Meng, S. Qin, L. Zhou, S. Li, H. Zhuo, G. Yang, Z.-G. Zhang, H. Ade, Y. Li, *Adv. Mater.* **2022**, 34, 2108749.

41. X. Xiong, X. Xue, M. Zhang, T. Hao, Z. Han, Y. Sun, Y. Zhang, F. Liu, S. Pei, L. Zhu, *ACS Energy Lett.* **2021**, 6, 3582.

42. Q. Wu, W. Wang, Y. Wu, R. Sun, J. Guo, M. Shi, J. Min, *Nati. Sci. Rev.* **2022**, 9, nwab151.

43. J.-W. Lee, C. Lim, S.-W. Lee, Y. Jeon, S. Lee, T.-S. Kim, J.-Y. Lee, B. J. Kim, *Adv. Energy Mater.* **2022**, n/a, 2202224.

44. J. Wang, C. Han, F. Bi, D. Huang, Y. Wu, Y. Li, S. Wen, L. Han, C. Yang, X. Bao, J. Chu, *Energy Environ. Sci.* **2021**, 14, 5968.

45. J. Huang, Z. Ren, Y. Zhang, P. W.-K. Fong, H. T. Chandran, Q. Liang, K. Yao, H. Tang, H. Xia, H. Zhang, X. Yu, Z. Zheng, G. Li, *Adv. Energy Mater.* **2022**, 12, 2201042.

This article is protected by copyright. All rights reserved.

15214095, ja, Downloaded from https://onlinelibrary.wiley.com/doi/10.1002/adma.202212275 by Hong Kong Poly University, Wiley Online Library on [10/02/2023]. See the Terms and Conditions (https://onlinelibrary.wiley.com/terms-and-conditions) on Wiley Online Library for rules of use; OA articles are governed by the applicable Creative Commons License

Accepted Article

46. J. Wang, C. Han, J. Han, F. Bi, X. Sun, S. Wen, C. Yang, C. Yang, X. Bao, J. Chu, *Adv. Energy Mater.* **2022**, 12, 2201614.

47. J. Han, F. Bao, D. Huang, X. Wang, C. Yang, R. Yang, X. Jian, J. Wang, X. Bao, J. Chu, *Adv. Funct. Mater.* **2020**, 30, 2003654.

48. C. Li, J. Zhou, J. Song, J. Xu, H. Zhang, X. Zhang, J. Guo, L. Zhu, D. Wei, G. Han, J. Min, Y. Zhang, Z. Xie, Y. Yi, H. Yan, F. Gao, F. Liu, Y. Sun, *Nat. Energy* **2021**, 6, 605.

49. J. Rivnay, S. C. B. Mannsfeld, C. E. Miller, A. Salleo, M. F. Toney, *Chem. Rev.* **2012**, 112, 5488.

50. X. Jiang, P. Chotard, K. Luo, F. Eckmann, S. Tu, M. A. Reus, S. Yin, J. Reitenbach, C. L. Weindl, M. Schwartzkopf, S. V. Roth, P. Müller-Buschbaum, *Adv. Energy Mater.* **2022**, 12, 2103977.

51. T. Duan, Q. Chen, D. Hu, J. Lv, D. Yu, G. Li, S. Lu, *Trends in Chemistry* **2022**, 4, 773.

52. Q. Bai, Q. Liang, H. Li, H. Sun, X. Guo, L. Niu, *Aggregate* **2022**, n/a, e281.

53. Z. Li, Y. Liang, X. Qian, L. Ying, Y. Cao, *Chem. Eng. J.* **2022**, 446, 136877.

54. Z. Liang, M. Li, Q. Wang, Y. Qin, S. J. Stuard, Z. Peng, Y. Deng, H. Ade, L. Ye, Y. Geng, *Joule* **2020**, 4, 1278.

55. Z. Wang, Z. Peng, Z. Xiao, D. Seyitliyev, K. Gundogdu, L. Ding, H. Ade, *Adv. Mater.* **2020**, 32, 2005386.

56. P. Müller-Buschbaum, *Adv. Mater.* **2014**, 26, 7692.

57. Q. Zhu, J. Xue, G. Lu, B. Lin, H. B. Naveed, Z. Bi, G. Lu, W. Ma, *Nano Energy* **2022**, 97, 107194.

58. N. Schopp, H. M. Luong, B. R. Luginbuhl, P. Panoy, D. Choi, V. Promarak, V. V. Brus, T.-Q. Nguyen, *ACS Energy Lett.* **2022**, 7, 1626.

59. T. A. Dela Peña, J. I. Khan, N. Chaturvedi, R. Ma, Z. Xing, J. Gorenflot, A. Sharma, F. L. Ng, D. Baran, H. Yan, F. Laquai, K. S. Wong, *ACS Energy Lett.* **2021**, 6, 3408.

60. S.-i. Natsuda, T. Saito, R. Shirouchi, Y. Sakamoto, T. Takeyama, Y. Tamai, H. Ohkita, *Energy Environ. Sci.* **2022**, 15, 1545.

This article is protected by copyright. All rights reserved.

15214095, ja, Downloaded from https://onlinelibrary.wiley.com/doi/10.1002/adma.202212275 by Hong Kong Poly University, Wiley Online Library on [10/02/2023]. See the Terms and Conditions (https://onlinelibrary.wiley.com/terms-and-conditions) on Wiley Online Library for rules of use; OA articles are governed by the applicable Creative Commons License

Accepted Article

61. S. Hultmark, S. H. K. Paleti, A. Harillo, S. Marina, F. A. A. Nugroho, Y. Liu, L. K. E. Ericsson, R. Li, J. Martín, J. Bergqvist, C. Langhammer, F. Zhang, L. Yu, M. Campoy-Quiles, E. Moons, D. Baran, C. Müller, *Advanced Functional Materials* **2020**, 30, 2005462.

62. Z. Wang, K. Gao, Y. Kan, M. Zhang, C. Qiu, L. Zhu, Z. Zhao, X. Peng, W. Feng, Z. Qian, X. Gu, A. K. Y. Jen, B. Z. Tang, Y. Cao, Y. Zhang, F. Liu, *Nat. Commun.* **2021**, 12, 332.

In a high-efficiency ternary matrix platform for all-polymer solar cells, the operational stability enhancement strategy is proposed with carefully studied underlying reasons, in terms of morphology and photo-physics. Based on the “cancelling-out” phenomenon, further ternary OPV blend design can be nourished by considering this principle during material combination, which could be useful in boosting both PCE and stability.

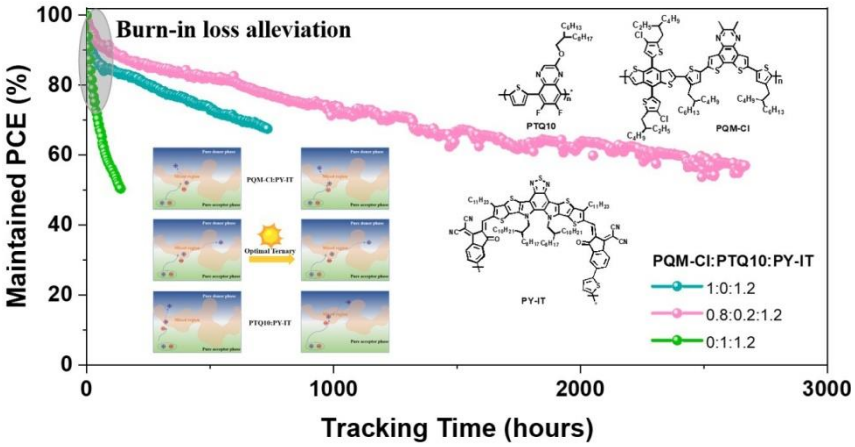

This article is protected by copyright. All rights reserved.

15214095, ja, Downloaded from https://onlinelibrary.wiley.com/doi/10.1002/adma.202212275 by Hong Kong Poly University, Wiley Online Library on [10/02/2023]. See the Terms and Conditions (https://onlinelibrary.wiley.com/terms-and-conditions) on Wiley Online Library for rules of use; OA articles are governed by the applicable Creative Commons License